# Generalization of the Ehrenfest urn model to a complex network

Jaime Clark,[1] Miguel Kiwi,[1,2] Felipe Torres,[1,2] José Rogan,[1,2] and Juan Alejandro Valdivia[1,2]
[1]*Departamento de Física, Facultad de Ciencias, Universidad de Chile, Santiago, Chile*
[2]*Centro para el Desarrollo de la Nanociencia y Nanotecnología, CEDENNA, Santiago, Chile*
(Received 9 January 2015; revised manuscript received 30 April 2015; published 6 July 2015)

The Ehrenfest urn model is extended to a complex directed network, over which a conserved quantity is transported in a random fashion. The evolution of the conserved number of packets in each urn, or node of the network, is illustrated by means of a stochastic simulation. Using mean-field theory we were able to compute an approximation to the ensemble-average evolution of the number of packets in each node which, in the thermodynamic limit, agrees quite well with the results of the stochastic simulation. Using this analytic approximation we are able to find the asymptotic dynamical state of the system and the time scale to approach the equilibrium state, for different networks. The study is extended to large *scale-free* and *small-world* networks, in which the relevance of the connectivity distribution and the topology of the network for the distribution of time scales of the system is apparent. This analysis may contribute to the understanding of the transport properties in real networks subject to a perturbation, e.g., the asymptotic state and the time scale required to approach it.

DOI: 10.1103/PhysRevE.92.012103 PACS number(s): 02.50.Ey, 05.10.Gg, 05.40.−a

## I. INTRODUCTION

The "Ehrenfest urn" has been a wonderful tool in the discussion and understanding of the basis of statistical mechanics for over a hundred years. Put forward by Ehrenfest and Ehrenfest [1] in 1907, it was solved exactly by Kac [2] 40 years later. Kac moreover referred to the Ehrenfest urn as "probably one of the most instructive models in the whole of physics" [3]. This is not only due to the fact that it could be solved exactly, but also because it allowed the clarification of such basic issues as the relation between the reversibility of the equations of motion of classical mechanics and the irreversibility of thermodynamics, notions put forward, although not fully understood, by Boltzmann in 1872, with the formulation of the $H$ theorem.

The original model put forward by the Ehrenfests consists in a stochastic process where $P$ marbles are initially placed in one urn and $N - P$ in another, with the marbles labeled from 1 to $N$. In each step of the dynamic process an integer $1 \leqslant n \leqslant N$ is chosen at random, with probability $1/N$, and the corresponding marble moved from one urn to the other. This model is popularly referred to as "fleas and dogs." Kac [2] was able to obtain the relaxation "time" for the system to reach equilibrium, the fluctuations, and the length of the Poincaré cycle. Already in 1968 Iglehart [4] successfully generalized these studies to Ehrenfest multiurn systems, and suggested interesting applications. In 2006 Flajolet *et al.* [5] proved that all balanced urn processes with two color balls (i.e., where the total number of balls added at any instant is a deterministic quantity) are analytically solvable in finite terms.

On the other hand, complex networks have attracted much attention in recent years, because they provide a useful representation for many technological, biological, and social systems of great applied and basic relevance [6–9]. For example, the internet and the World Wide Web (www) are complex networks connected by either physical or virtual links. The cell may be envisioned as a network of molecules connected by their interactions and reactions. Knowledge itself might be construed as an enormously complex network of humans, connected by gesture, voice, and writing. Consequently, the topology and dynamics of complex networks have motivated the scientific community to the quest for an understanding of their structure and mechanisms.

Many of these networks have common features, such as the connectivity distribution $P(k)$, where $k$ is the average number of links per node, which often behaves [10–19] as a power law $P(k) \sim k^{-\alpha}$ for large $k$ values, in the so-called *scale-free networks*. Several authors have developed network models that seek to replicate these distributions. One of the most emblematic cases was proposed by Barabási and Albert [6,20,21], in which a weighted random growth model is used to generate a power-law distribution with $\alpha = 3.0$. In this model, in each step a new vertex appears, which is connected randomly with a vertex of the network with a probability proportional to its connectivity degree. Empirical networks have a similar characteristic exponent; examples are citation networks [10] and electronics circuits [11]. However, there are other important systems which exhibit a network structure with a different exponent, for example, telephone calls [12,13], the World Wide Web [14], metabolism [15], movie actors [16], protein interactions [17], the internet [18], and word co-occurrence [19], among others. In these cases, the characteristic exponent ranges from 2.0 to 2.7. There are also models of preferential attachment, which produce different link distributions and network structures on changing a parameter [22].

There has been a growing interest in studying the evolution of these networks [8,9,23], and more recently, researchers have become interested in studying the network as a dynamical system in which a given object can be transported across the network, such as the propagation of rumors, infections [24,25], information packets [26,27], cars [28–31], buses [32,33], water [34], trains [35], citations [10], sand [36,37], earthquakes [38], etc. In this context, it has become of interest to study the distribution of the distances between nodes (as the shortest path along the network). Noteworthy examples are large networks with a small average distance, the so-called *small-world networks* of Watts and Strogatz [23]. It is expected that the average distance and the topology should control the transport time scale distribution in these networks.

In this work we present a generalization of the Ehrenfest model in which a number of urns are interconnected as a

 ©2015 American Physical Society

complex network, and the marbles or packets can jump only to urns with which the first one has a directed connection. A complex network of Ehrenfest urns thus describes the transport of a conserved quantity through the network, which shares similarities with networks such as traffic in cities, electric networks, etc. A few attempts in this direction have been reported in the literature. For example, it is worth mentioning the treatment of $M$ urns on a circular ring, with periodic boundary conditions [39–42]. In our case, we apply a mean-field approach to obtain the relaxation "time" of the system, and the extension to the time evolution of each node, for an arbitrary number of urns and an arbitrary topology of their links. The analytical expressions are successfully compared with the stochastic simulation results. The analysis is applied to networks of different sizes.

This paper is divided as follows: In Sec. II, we present the details of the problem. In Sec. III we describe the mean-field solution and compare this solution for small simple networks with stochastic simulations of the system. In Sec. IV we consider networks of different sizes. In Sec. V we summarize and draw conclusions.

## II. MODEL

The Ehrenfest urn describes the transport of a conserved quantity (marbles or packets) between two nodes (or urns) that are directly connected and at time $t$ have $m_1(t) = n$ and $m_2(t) = N - n$ packets, respectively. Here $m_i(t)$ is the number of packets at the $i$th node. At this time $t$, one of these $N$ packets, chosen at random, is transported from the original node $(i)$ to another node $(j)$. Hence, the number of packets at node $\ell$ changes to

$$m_\ell(t+1) = m_\ell(t) + \Delta_\ell^{(i,j)}. \tag{1}$$

For example, if a packet is chosen from the first node, we have $\Delta_1^{(1,2)} = -1$ and $\Delta_2^{(1,2)} = 1$. Similarly, if a packet is chosen from the second node, we have $\Delta_1^{(2,1)} = 1$ and $\Delta_2^{(2,1)} = -1$. The procedure is then repeated in time. As mentioned above, the analytic solution of this stochastic model was accomplished by Kac [2].

In order to generalize this model to a complex network, we consider a set of $M$ nodes, each with $m_i(t)$ packets, such that at all times we have a total of

$$N = \sum_{i=1}^{M} m_i(t) \tag{2}$$

packets. A particular node $i$ is connected to $k_i$ nodes (*out degree*), and the packets in the $i$th node can move only to the $k_i$ nodes to which it is connected (its *outgoing set*). An example of a three-node network, in which the arrows determine the directed connectivity of the network, is shown in Fig. 1(a). We can define the adjacency matrix $\mathbf{A}$ of this network, with elements $A_{i,j} = 1$ if there is a directed connection from node $i$ to node $j$ and 0 otherwise, namely,

$$\mathbf{A} = \begin{bmatrix} 0 & 1 & 1 \\ 1 & 0 & 0 \\ 0 & 1 & 0 \end{bmatrix}. \tag{3}$$

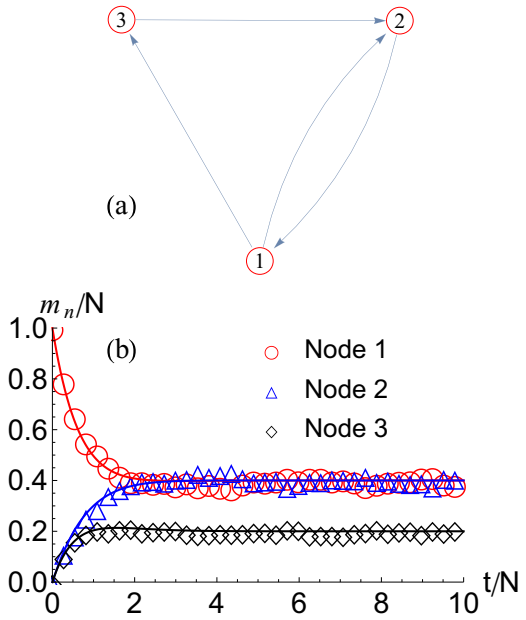


FIG. 1. (Color online) (a) Three-node network, in which the arrows determine the directed connectivity of the network. (b) Evaluation of the number of packets at each node as a function of time, $m_i(t)$ for $i = 1$, 2, and 3, corresponding to the red circles, blue triangles, and black diamond symbols, respectively. For comparison we also show the evolution obtained from a stochastic simulation (symbols) and the results of the analytical solution (solid lines). The initial conditions are $m_1(0) = N = 1000$, $m_2(0) = m_3(0) = 0$.

With this notation, we can calculate the connectivity of the $i$th node (the number of nodes to which it is connected) as

$$k_i = \sum_j A_{i,j}. \tag{4}$$

The time evolution is similar to that given by Eq. (1), namely, at time $t$ we choose one of the $N$ packets, let us say it happens to be from node $i$, and then we choose one of the $k_i$ nodes in its *outgoing set*, let us say node $j$. The evolution of the number of packets on each node becomes

$$\Delta_\ell^{(i,j)} = \begin{cases} -1, & \ell = i, \\ +1, & \ell = j, \\ 0, & \ell \neq i,\ \ell \neq j. \end{cases} \tag{5}$$

For simplicity we run a stochastic simulation of this three-node network with the initial conditions $m_1(0) = N = 1000$, $m_2(0) = m_3(0) = 0$. We see from Fig. 1(b) that, within the expected stochastic fluctuations, the system reaches an asymptotic solution for large times, which fluctuates around $\langle m_1 \rangle \approx \langle m_2 \rangle \approx 2N/5$ and $\langle m_3 \rangle \approx N/5$. We will show below how to obtain this asymptotic state analytically from our mean-field approach.

For the sake of completeness we consider the symmetric network of Fig. 2(a), which has the adjacency matrix

$$\mathbf{A} = \begin{bmatrix} 0 & 1 & 1 \\ 1 & 0 & 1 \\ 1 & 1 & 0 \end{bmatrix}. \tag{6}$$

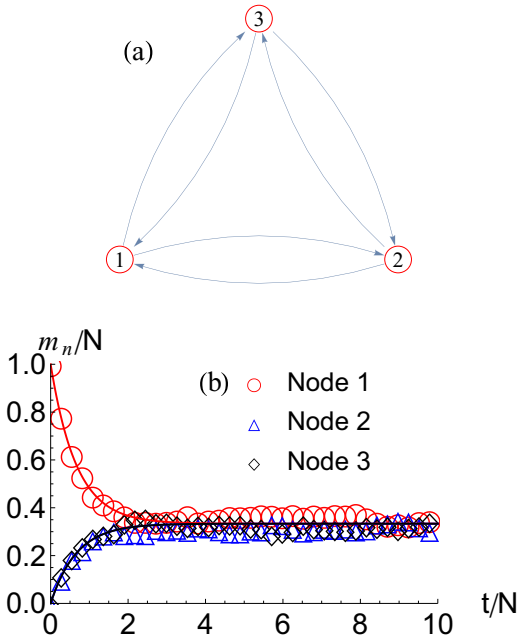


FIG. 2. (Color online) (a) Three-node network, in which the arrows determine the directed connectivity of the network. (b) Evaluation of $m_i(t)$ for $i = 1$ (red circles), 2 (blue triangles), and 3 (black diamonds). The continuous lines correspond to the analytic mean-field solution and the symbols to the stochastic solution. The initial conditions are $m_1(0) = N = 1000$, $m_2(0) = m_3(0) = 0$.

The evolution in this case, from the same initial condition $m_1(0) = N = 1000$, $m_2(0) = m_3(0) = 0$, converges asymptotically to $\langle m_1\rangle \approx \langle m_2\rangle \approx \langle m_3\rangle \approx N/3$, as expected for a symmetric situation. It is interesting to notice that the connectivity, as described by the adjacency matrix, determines the time scales of the system and its asymptotic behavior. We will show below that, within a mean-field approach, the above-mentioned asymptotic results are indeed exact in the $t \to \infty$ limit.

## III. MEAN-FIELD APPROACH

In a mean-field approach, one assumes that evaluating an ensemble-average evolution $\langle m_i(t)\rangle$ of $m_i(t)$, in the thermodynamic limit, is equivalent to assuming that all the $N$ packets move to a new node in a time $N$, so that the evolution equation for the ensemble average is

$$\langle m_i(t+1)\rangle - \langle m_i(t)\rangle \approx \frac{1}{N}\left(-\langle m_i(t)\rangle + \sum_{j\neq i}^{N} \frac{A_{ji}}{k_j}\langle m_j(t)\rangle\right). \tag{7}$$

Intuitively we know that after $N$ steps, on average, the packets in node $j$ move in the same proportion to all nodes of its outgoing set of size $k_j$, so that each one receives on average $\langle m_j/k_j\rangle$ packets. In this process, the $i$th node will receive these $\langle m_j/k_j\rangle$ packets only if the $j$th node is connected to the $i$th node, namely, if $A_{j,i} = 1$. At the same time all of the packets in the $i$th node will move to the $k_i$ nodes in the outgoing set of the $i$th node.

We approximate the left-hand side of the above equation as a time derivative, namely, as

$$\langle m_i(t+1)\rangle - \langle m_i(t)\rangle \approx \frac{d}{dt}\langle m_i(t)\rangle, \tag{8}$$

so that the evolution equation can be approximated as

$$\frac{d}{dt}\langle m_i(t)\rangle = \frac{1}{N}\left(-\langle m_i(t)\rangle + \sum_{j\neq i}^{n} \frac{A_{ji}}{k_j}\langle m_j(t)\rangle\right). \tag{9}$$

All of these approximations improve as we approach the thermodynamic limit ($N \to \infty$), as the deviations become relatively small, and the time derivative becomes a more accurate approximation due to the $N^{-1}$ factor in Eq. (9). The mean-field approach gives us a simple closed-form expression for the evolution of the ensemble average $\langle m_i(t)\rangle$. However, we relinquish the possibility of evaluating the amplitude of the fluctuations, which in general require one to obtain the evolution of a master equation, which we will give in a future presentation.

The above system of equations can be written in vector form as

$$\frac{d}{dt}\langle \vec{\mathbf{m}}(t)\rangle = \frac{1}{N}\mathbf{B}\,\langle \vec{\mathbf{m}}(t)\rangle, \tag{10}$$

where $\langle \vec{\mathbf{m}}(t)\rangle \to \{\langle m_1(t)\rangle, \langle m_2(t)\rangle, \ldots, \langle m_M(t)\rangle\}$, and $\mathbf{B}$ is the dynamical matrix whose elements are

$$B_{i,j} = -\delta_{i,j} + \frac{A_{j,i}}{k_j}, \tag{11}$$

where $\delta_{i,j}$ is the Kronecker delta. The formal solution to Eq. (10) is

$$\langle \vec{\mathbf{m}}(t)\rangle = e^{\mathbf{B}t/N}\,\langle \vec{\mathbf{m}}(0)\rangle, \tag{12}$$

which can be obtained by diagonalizing the dynamical matrix $\mathbf{B}$, such that

$$\mathbf{B} = \mathbf{V}^{-1}\Lambda\mathbf{V}, \tag{13}$$

and writing

$$\langle \vec{\mathbf{m}}(t)\rangle = \mathbf{V}^{-1}\, e^{\Lambda t/N}\, \mathbf{V}\, \langle \vec{\mathbf{m}}(0)\rangle, \tag{14}$$

where $\Lambda$ is the diagonal matrix of the eigenvalues $\{\lambda_1, \lambda_2, \ldots, \lambda_M\}$ of $\mathbf{B}$, and $\mathbf{V}$ is the matrix of column eigenvectors.

The matrix represented by $A_{j,i}/k_j$ in Eq. (9) is called a stochastic or Markov matrix, since it has non-negative terms and its columns add up to 1. Furthermore, it can be checked that its maximum eigenvalue $\lambda_{\max} = 1$. Hence, the matrix $\mathbf{B}$ has a maximum eigenvalue $\lambda_{\max} = 0$, so that the system is stable and eventually converges asymptotically to a steady state. This is expected since the above system conserves the total number of packets, namely,

$$\sum_{i=1}^{M}\langle m_i(t)\rangle = N. \tag{15}$$

It is interesting to notice that if we apply this procedure to the original Ehrenfest urn, we can write the adjacency and

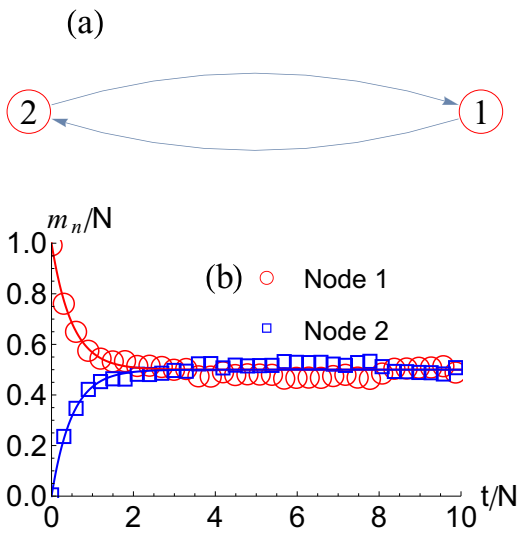


FIG. 3. (Color online) (a) The two-node network corresponding to the original Ehrenfest urn. (b) Evaluation of $m_i(t)$ for $i = 1$ (red circles) and 2 (blue squares). The continuous lines correspond to the analytic mean-field solution and the symbols to a stochastic simulation. The initial conditions are $m_1(0) = N = 1000, m_2(0) = 0$.

dynamical matrices as

$$\mathbf{A} = \begin{bmatrix} 0 & 1 \\ 1 & 0 \end{bmatrix} \tag{16}$$

and

$$\mathbf{B} = \begin{bmatrix} -1 & 1 \\ 1 & -1 \end{bmatrix}, \tag{17}$$

respectively. The eigenvalues of $\mathbf{B}$ are $\lambda_1 = -2$ and $\lambda_0 = 0$, with the corresponding eigenvectors $\vec{v}_1 = \{-1,1\}/2$ and $\vec{v}_0 = \{1,1\}/2$, respectively. The solution of the matrix exponentiation is

$$\begin{aligned} \langle m_1(t)\rangle &= Ne^{-t/N}\cosh(t/N), \\ \langle m_2(t)\rangle &= Ne^{-t/N}\sinh(t/N), \end{aligned} \tag{18}$$

assuming the initial condition $\langle m_1(0)\rangle = N$ and $\langle m_2(0)\rangle = 0$. The asymptotic state can be read directly from the solution, or from the eigenvector corresponding to the $\lambda_0 = 0$ eigenvalue, namely, $\{\langle m_1\rangle, \langle m_2\rangle\} = N\vec{v}_0 = \{N/2, N/2\}$. The time evolution is given in Fig. 3. The relaxation time $\tau$ required to converge to the asymptotic state corresponds to the real part of the smallest nonzero eigenvalue (the negative of its real part), namely,

$$\tau = -N\mathrm{Re}\left[\lambda_1^{-1}\right] = N/2, \tag{19}$$

which can also be obtained directly from the solution. These results agree with the original Kac solution to the Ehrenfest model [2], in the thermodynamic limit.

For the three-node asymmetric network presented in the previous section, we have

$$\mathbf{B} = \begin{bmatrix} -1 & 1 & 0 \\ \frac{1}{2} & -1 & 1 \\ \frac{1}{2} & 0 & -1 \end{bmatrix}. \tag{20}$$

The eigenvalues are $\lambda_\pm = (-3 \pm i)/2$, and $\lambda_0 = 0$. The eigenvector corresponding to $\lambda_0 = 0$ is $\vec{v}_0 = \{2,2,1\}/5$, so that the asymptotic state is $\langle m_1\rangle = \langle m_2\rangle = 2N/5$ and $\langle m_3\rangle = N/5$, as discussed in the previous section. The analytical solution is presented in Fig. 1(b), showing that it agrees well with the solution obtained from the stochastic simulations. The relaxation time $\tau$ required to converge to the asymptotic state is given by Eq. (19) as $\tau = 2N/3$, which also can be obtained directly from the solution.

Similarly, for the three-node symmetric network presented in the previous section, we have

$$\mathbf{B} = \begin{bmatrix} -1 & \frac{1}{2} & \frac{1}{2} \\ \frac{1}{2} & -1 & \frac{1}{2} \\ \frac{1}{2} & \frac{1}{2} & -1 \end{bmatrix}. \tag{21}$$

The eigenvalues are $\lambda_{1,2} = 3/2$ and $\lambda_0 = 0$. The eigenvector corresponding to $\lambda_0 = 0$ is $\vec{v}_0 = [1,1,1]/3$, so that the asymptotic state is $\langle m_1\rangle = \langle m_2\rangle = \langle m_3\rangle = N/3$, as was discussed in the previous section. The analytical solution is presented in Fig. 2(b) and agrees quite well with the solution obtained from the stochastic simulations. The relaxation time $\tau$ required to converge to the asymptotic state corresponds to $\tau = -N\mathrm{Re}[\lambda_{1,2}^{-1}] = 2N/3$, which is identical to the asymmetric three-node network.

Hence we notice that in the thermodynamic limit, namely, for large $N$, the analytic mean-field solution does represent quite well the mean behavior of the "Ehrenfest" network. Furthermore, since the asymptotic dynamical state is represented by the $\lambda_0 = 0$ eigenstate of the $\mathbf{B}$ matrix, it becomes clear that the asymptotic state is a global characteristic of the network as a whole. Thus, understanding such an asymptotic state provides information about the structure of the network.

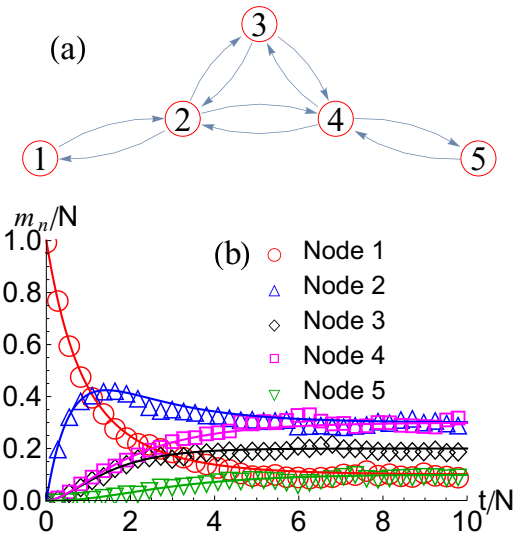


FIG. 4. (Color online) (a) Five-node network, in which the arrows determine the directed connectivity of the network. (b) Evaluation of $m_i(t)$ for $i = 1$ (red circles), 2 (blue triangles), 3 (dark-green diamonds), 4 (magenta squares), and 5 (light-green inverted triangles). We show both the mean-field theory analytic solution (solid lines) and results of the stochastic simulation (symbols). The initial conditions are $m_1(0) = N = 1000, m_2(0) = m_3(0) = m_4(0) = m_5(0) = 0$.

To demonstrate the strength of the analytical mean-field solution we analyze the five-node network shown in Fig. 4(a), which yields a nontrivial behavior for one of the nodes. In this case the eigenvalues are $\lambda_{\pm} = (-7 \pm \sqrt{13})/6$, $\lambda_3 = -10/6$, $\lambda_4 = -1$, $\lambda_0 = 0$. The eigenvector corresponding to $\lambda_0 = 0$ is $\vec{v}_0 = \{1,3,2,3,1\}/10$, so that the asymptotic state is $\langle m_1 \rangle = \langle m_5 \rangle = N/10$, $\langle m_2 \rangle = \langle m_4 \rangle = 3N/10$, and $\langle m_3 \rangle = 2N/10$. The relaxation time $\tau$ required to converge to the asymptotic state is $\tau = -N\mathrm{Re}[\lambda_4^{-1}] = 1.767\,59$.

## IV. LARGER NETWORKS

We now turn our attention to the dynamics of larger $M$-node networks, by considering the time-scale distribution of *small-world* and *scale-free* networks.

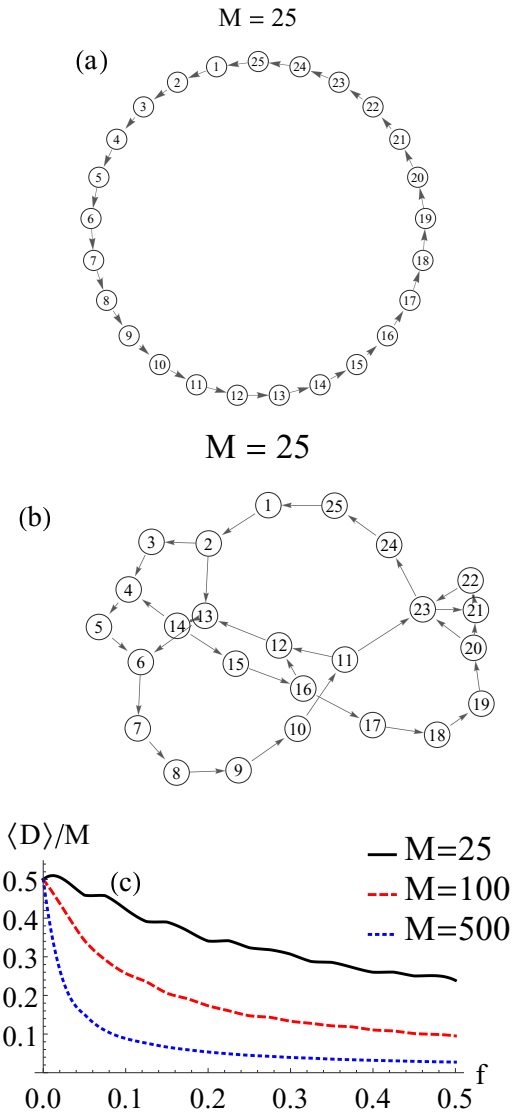


FIG. 5. (Color online) (a) $M = 25$-node ring network, in which the arrows determine the directed connectivity of the network. (b) 25-node small-world network with connection probability $f = 0.3$. (c) The average normalized distance $\langle D \rangle / M$ as a function of $f$, for $M = 25$ (solid black), $M = 100$ (dashed red), and $M = 500$ (dotted blue) nodes. The average is taken over an ensemble of 50 realizations.

To construct the small-world networks of Watts and Strogatz [23] we start with a ring network of $M$ nodes, as shown in Fig. 5(a), and then connect $M \times f$ distinct pairs of nodes, as shown in Fig. 5(b) for $f = 0.3$. These networks are called small-world networks because the average distance $\langle D \rangle / M$ between nodes decreases with $f$, as shown in Fig. 5(c). The distance between nodes $i$ and $j$ is defined as the minimum

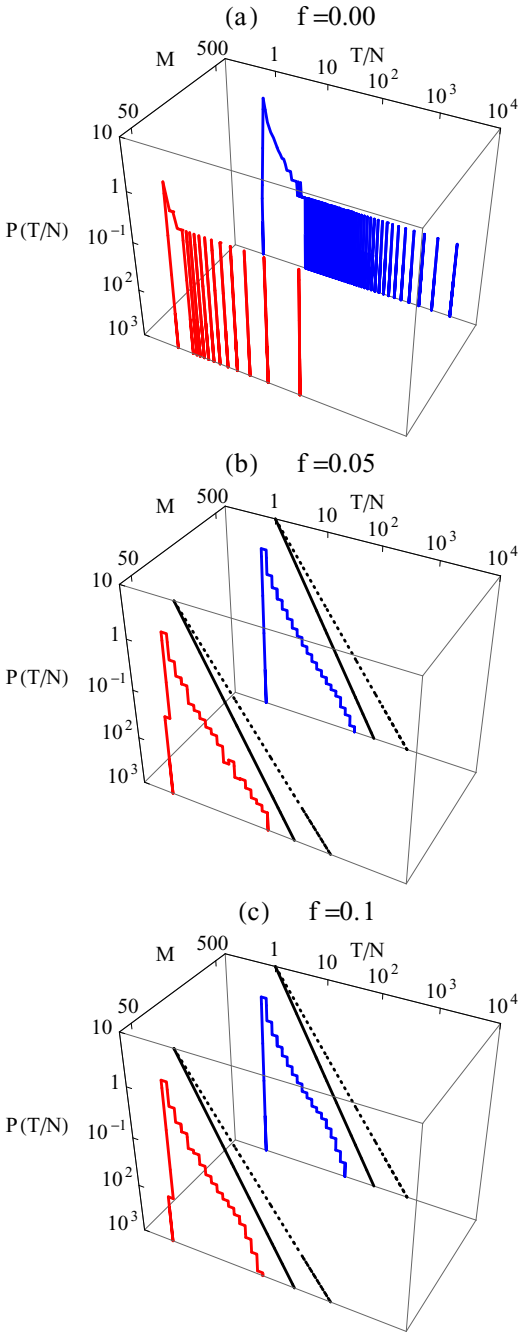


FIG. 6. (Color online) The distribution of time scales for the small-world networks: (a) ring network ($f = 0$), (b) $f = 0.05$ network, and (c) $f = 0.1$ network. We show the distribution for $M = 50$ (solid red) and $M = 500$ (dashed blue) nodes. The distribution is constructed from 500 and 50 realizations, respectively, for each size. As a reference we also show the $T^{-2}$ scaling (solid black line) and the $T^{-1.5}$ scaling (dotted black line), for $f = 0.05$ and 0.1.

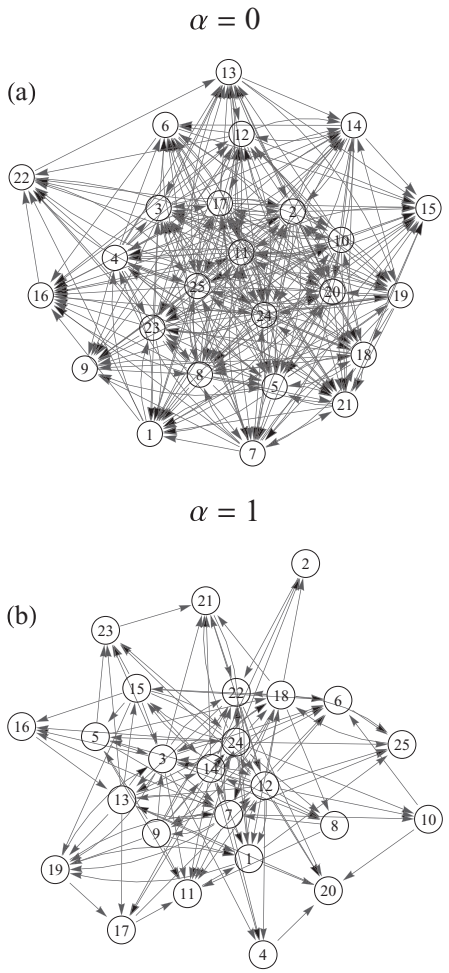


FIG. 7. $M = 25$-node scale-free network, in which the arrows determine the directed connectivity of the network, for (a) $\alpha = 0$ and (b) $\alpha = 1.0$.

number of steps required to reach node $j$ from node $i$ along the network, and considering the directed nature of the network. The normalization in the figure is adopted because for $f = 0$ we have $\langle D \rangle = M/2$.

In Fig. 6 we compute the distribution of time scales, defined as the inverse of the real part of the eigenvalues of the **B** matrix for the network. Of course, we do not consider the $\lambda_0 = 0$ eigenvalue. In Fig. 6(a), we show the distribution of time scales for the ring network, corresponding to $f = 0$. We notice that, as $M$ increases, the maximum time scale also increases (vertical lines). In fact, for $f = 0$ the largest time scale grows as $T \sim M^2 N$, which in some way represents metastable states which are different from the asymptotic solution represented by the $\lambda_0 = 0$ state, which has an infinite time scale. Their characterization will be provided elsewhere. The distribution of the shorter time scales seems to follow a $\sim T^{-1.5}$ power law. In Figs. 6(b) and 6(c) we notice that these metastable states disappear, so that they are the singular solutions for the $f = 0$ ring network. The distribution for the shorter time scales continues to follow a $\sim T^{-1.5}$ power law, as in the $f = 0$ case.

Now we compare the previous results with the distribution of time scales for scale-free networks, which have a power-law

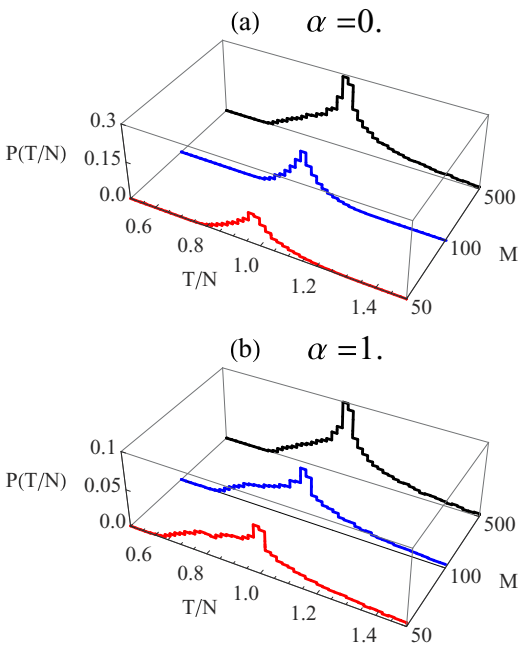


FIG. 8. (Color online) The distribution of time scales for the scale-free networks with (a) $\alpha = 0$ and (b) $\alpha = 1.0$. We show the distributions for $M = 50$ (red), $M = 100$ (blue), and $M = 500$ (black). The distributions are constructed from 500, 250, and 50 realizations for each size, respectively.

distribution of links, or in our case of *outgoing degrees*. We notice from Eq. (11) that it is fairly easy to construct the matrix **B** with a given distribution of the *outgoing degree* $k$, from the adjacency matrix **A**. Indeed, for each element $k_i$ of the set $\{k_i : i = 1, \ldots, N-1\}$ of *outgoing degrees*, we choose a random set of $k_i$ different integers $1 \leqslant x_j^{(i)} \leqslant N$ to which node $i$ is connected with the restriction that $x_j^{(i)} \neq i$. With these $x_j^{(i)}$ we fill with 1's the corresponding elements of the $i$th row of the matrix **A**.

We use a power-law distribution of links, given by $P(k) \sim k^{-\alpha}$, and where $\alpha = 0$ means a uniform distribution, which produces a network of the type shown in Fig. 7(a). We notice that the average number of links is determined by the value of $\alpha$ as

$$\langle k \rangle = \frac{\sum_{n=1}^{N-1} n^{1-\alpha}}{\sum_{n=1}^{N-1} n^{-\alpha}}. \tag{22}$$

In general, the number of links decreases as we increase $\alpha$, as can be seen by comparing Fig. 7(a) and Fig. 7(b), for $\alpha = 0$ and $\alpha = 1$, respectively.

We can compute the distribution of time scales for these networks, as shown in Fig. 8. Results for the uniform distribution ($\alpha = 0$) of directed links are shown in Fig. 8(a) for $M = 50$, 100, and 500 nodes. We observe that the three distributions are somewhat different. The time scales for larger $M$ become concentrated close to $T/N \sim 1$ with a narrower distribution. In a network with a uniform link distribution, the average connectivity with the other nodes is $M/2$, so that the connectivity is fairly large compared to larger $\alpha$ values (and small small-world networks with small $f \ll 1$ values). The $\alpha = 1.0$ case is shown in Fig. 8(b). As we increase $\alpha$ the

average number of directed links is reduced, so that $\langle k \rangle \approx 11$, 19, and 73 for $M = 50$, 100, and 500, respectively, for $\alpha = 1$. The time-scale distribution widens as we increase $\alpha$, as it takes more time for the system to converge to a steady state. Therefore, the connectivity distribution and the topology in general change the distribution of time scales. Its detailed characterization will be presented elsewhere.

## V. SUMMARY

We have generalized the Ehrenfest urn model to a complex network of urns, in which the packets or marbles move from node to node following the network connections. We have obtained an analytical solution for the ensemble-average evolution of the number of packets in each node, implementing a mean-field approach in the thermodynamic limit (namely, $N \gg 1$). With this solution we not only find the ensemble-average evolution of $m_i(t)$, but we also evaluate analytically the asymptotic steady-state solution and the relaxation time $\tau$ to reach such solution.

This analysis allows for the possibility to investigate larger networks and to study the distribution of time scales produced by the network and the characteristic time scale (relaxation time) required by the system to reach the asymptotic dynamical state. Both small scale-free and small-world networks have been studied. We observe that the connectivity distribution, and the topology in general, change the distribution of time scales.

When the perturbations become time dependent, it may be of interest to study the resonant behavior of the system, as the external driver may resonate with some of its natural time scales. We will analyze these issues in a future presentation.

Since the analysis considers the random transport of a conserved quantity through the network, it is expected that our results could be useful to understand how packets can be transported randomly through an arbitrary network, and how a steady-state situation is reached after a perturbation is imposed. Of course, for the time being the results apply only to networks where the conserved quantity is transported randomly, but without losses, through the system.

## ACKNOWLEDGMENTS

This work was supported by the Fondo Nacional de Investigaciones Científicas y Tecnológicas (FONDECYT, Chile) under Grants No. 1120399 and No. 1130272 (M.K. and J.R.), and No. 1150718 (J.A.V.), and Financiamiento Basal para Centros Científicos y Tecnológicos de Excelencia No. FB0807.

[1] P. Ehrenfest and T. Ehrenfest, Physik **8**, 311 (1907).
[2] M. Kac, Am. Math. Mon. **54**, 369 (1947).
[3] M. Kac, *Probability and Related Topics in Physical Sciences*, Vol. 54, Am. Math. Monthly (Interscience Publishers, New York, NY, 1959).
[4] D. L. Iglehart, Ann. Math. Stat. **39**, 864 (1968).
[5] P. Flajolet, P. Dumas, and V. Puyhaubert, *Colloquium on Mathematics and Computer Science*, Discrete Mathematics and Theoretical Computer Science Proc. AG (DMTCS, Nancy, France, 2006), pp. 59–118.
[6] R. Albert and A.-L. Barabási, Rev. Mod. Phys. **74**, 47 (2002).
[7] M. E. J. Newman, SIAM Rev. **45**, 167 (2003).
[8] S. N. Dorogovtsev and J. F. F. Mendes, Adv. Phys. **51**, 1079 (2002).
[9] S. N. Dorogovtsev and J. F. F. Mendes, *Evolution of Networks: From Biological Nets to the Internet and WWW* (Oxford University Press, Inc., New York, NY, 2003).
[10] S. Redner, Eur. Phys. J. B **4**, 131 (1998).
[11] R. F. Cancho, C. Janssen, and R. V. Solé, Phys. Rev. E **64**, 046119 (2001).
[12] W. Aiello, F. Chung, and L. Lu, in *Proceedings of the 32nd Annual ACM Symposium on Theory of Computing* (ACM, New York, NY, USA, 2000), pp. 171–180.
[13] W. Aiello, F. Chung, and L. Lu, in *Handbook of Massive Data Sets*, edited by J. Abello, P. M. Pardalos, and M. G. C. Resende (Kluwer, Dordrecht, 2002), pp. 97–122.
[14] A. Broder, R. Kumar, F. Maghoul, P. Raghavan, S. Rajagopalan, R. Stata, A. Tomkins, and J. Wiener, Comput. Networks **33**, 309 (2000).
[15] H. Jeong, B. Tombor, R. Albert, Z. N. Oltvai, and A.-L. Barabási, Nature (London) **407**, 651 (2000).
[16] L. A. N. Amaral, A. Scala, M. Barthélémy, and H. E. Stanley, Proc. Natl. Acad. Sci. U.S.A. **97**, 11149 (2000).
[17] H. Jeong, S. P. Mason, A.-L. Barabási, and Z. N. Oltvai, Nature (London) **411**, 41 (2001).
[18] M. Faloutsos, P. Faloutsos, and C. Faloutsos, in *Proceedings of the Conference on Applications, Technologies, Architectures, and Protocols for Computer Communication* (ACM, New York, NY, 2000), pp. 251–262.
[19] R. F. Cancho and R. V. Solé, Proc. R. Soc. London, Ser. B **268**, 2261 (2001).
[20] A.-L. Barabási and R. Albert, Science **286**, 509 (1999).
[21] A. L. Barabási, L. Nitsch, and I. A. Dorobantu, Phys. Lett. A **139**, 53 (1989).
[22] A. Lipowski and D. Lipowska, Phys. Rev. E **90**, 032815 (2014).
[23] D. J. Watts and S. H. Strogatz, Nature (London) **393**, 440 (1998).
[24] F. Liljeros, C. R. Edling, and L. A. N. Amaral, Microbes Infect. **5**, 189 (2003).
[25] F. Liljeros, C. R. Edling, L. A. N. Amaral, H. E. Stanley, and Y. Aberg, Nature (London) **411**, 907 (2001).
[26] B. Tadic, G. J. Rodjers, and S. Thurner, Int. J. Bifurcation Chaos Appl. Sci. Eng. **17**, 2363 (2007).
[27] A. Farina, A. Graziano, F. Mariani, M. C. Recchioni, and F. Zirilli, Commun. Network **4**, 147 (2012).
[28] M. Barthélemy and A. Flammini, J. Stat. Mech. (2006) L07002.
[29] S. Lämmer, B. Gehlsen, and D. Helbing, Physics A **363**, 89 (2006).
[30] A. Varas, M. D. Cornejo, B. A. Toledo, V. Muñoz, J. Rogan, R. Zarama, and J. A. Valdivia, Phys. Rev. E **80**, 056108 (2009).
[31] F. Castillo, B. Toledo, V. Muñoz, J. Rogan, R. Zarama, M. Kiwi, and J. A. Valdivia, Physica A **403**, 65 (2013).

[32] T. Nagatani, Phys. Rev. E **68**, 036107 (2003).
[33] J. Villalobos, V. Muñoz, J. Rogan, R. Zarama, N. F. Johnson, B. Toledo, and J. A. Valdivia, Phys. Rev. E **89**, 062922 (2014).
[34] S. li Yang, N.-S. Hsu, P. W. F. Louie, and W. W.-G. Yeh, J. Infrastructure Syst. **2**, 54 (1996).
[35] P. Sen, S. Dasgupta, A. Chatterjee, P. A. Sreeram, G. Mukherjee, and S. S. Manna, Phys. Rev. E **67**, 036106 (2003).
[36] K.-I. Goh, D.-S. Lee, B. Kahng, and D. Kim, Phys. Rev. Lett. **91**, 148701 (2003).
[37] D. Lee, K.-I. Goh, B. Kahng, and D. Kim, Physica A **84**, 338 (2004).
[38] D. Pasten, V. Muñoz, A. Cisternas, J. Rogan, and J. A. Valdivia, Phys. Rev. E **84**, 066123 (2011).
[39] Y.-M. Kao and P.-G. Luan, Phys. Rev. E **67**, 031101 (2003).
[40] P.-G. Luan and Y.-M. Kao, Phys. Rev. E **69**, 022102 (2004).
[41] Y.-M. Kao, Phys. Rev. E **69**, 027103 (2004).
[42] A. Lipowski and M. Droz, Phys. Rev. E **65**, 031307 (2002).